

Multi-electron systems in strong magnetic fields II: A fixed-phase diffusion quantum Monte Carlo application based on trial functions from a Hartree-Fock-Roothaan method

S. Boblest^{a,*}, D. Meyer^a, G. Wunner^a

^a*Institut für Theoretische Physik I, Universität Stuttgart, 70550 Stuttgart, Germany*

Abstract

We have developed a quantum Monte Carlo application for the computation of energy eigenvalues for atoms and ions in strong magnetic fields. We use guiding wave functions obtained by Hartree-Fock-Roothaan calculations. For these calculations, we use previously published code C. Schimeczek, D. Engel, G. Wunner, *Comp. Phys. Comm.* 183, 1502 – 1510 (2012)], as well as the recently developed 2DLHFR method described in an accompanying publication.

Keywords: Neutron star magnetic fields; Atomic data; Quantum Monte Carlo

PROGRAM SUMMARY

Manuscript Title: Multi-electron systems in strong magnetic fields II: A fixed-phase diffusion quantum Monte Carlo application based on trial functions from a Hartree-Fock-Roothaan method from a Hartree-Fock-Roothaan method

Authors: S. Boblest, D. Meyer, G. Wunner

Program Title: Manteca

Journal Reference:

Catalogue identifier:

Licensing provisions:

Programming language: C++

Computer: Cluster of 1~500 HP Compaq dc5750

*Corresponding author.

E-mail address: Sebastian.Boblest@itp1.uni-stuttgart.de

Preprint submitted to Computer Physics Communications

February 27, 2014

Operating system: Linux

RAM: 500 MByte per node

Number of processors used: 1~1000

Keywords: neutron star magnetic fields, atomic data, quantum Monte Carlo

Classification: 2.1 Atomic Physics - Structure and Properties

External routines/libraries: Boost::Serialization, Boost::MPI, LAPACK SLATEC

Unusual features: The program needs approximate wave functions computed with another method as input.

Nature of problem:

Quantitative modellings of features observed in the X-ray spectra of isolated neutron stars are hampered by the lack of sufficiently large and accurate databases for atoms and ions up to the last fusion product iron, at high magnetic field strengths. The predominant amount of line data in the literature has been calculated with Hartree-Fock methods, which are intrinsically restricted in precision. Our code is intended to provide a powerful tool for calculating very accurate energy values from, and thereby improving the quality of, existing Hartree-Fock results.

Solution method:

The Fixed-phase quantum Monte Carlo method is used in combination with guiding functions obtained in Hartree-Fock calculations. The guiding functions are created from single-electron orbitals ψ_i which are either products of a wave function in the z -direction (the direction of the magnetic field) and an expansion of the wave function perpendicular to the direction of the magnetic field in terms of Landau states, $\psi_i(\rho, \varphi, z) = P_i(z) \sum_{n=0}^{N_L} t_{in} \phi_{ni}(\rho, \varphi)$, or a full two-dimensional expansion using separate z -wave functions for each Landau level, i.e. $\psi_i(\rho, \varphi, z) = \sum_{n=0}^{N_L} P_{ni}(z) \phi_{ni}(\rho, \varphi)$. In the first form, the t_{in} are expansion coefficients, and the expansion is cut off at some maximum Landau level quantum number N_L . In the second form, the expansion coefficients are contained in the respective P_{ni} .

Restrictions:

The method itself is very flexible and not restricted to a certain interval of magnetic field strengths. However, the HFFER II and 2DLHFR methods can only obtain guiding functions in the regime of strong magnetic fields.

Running time: 1 minute - several days

1. Introduction

The analysis of absorption features in the spectra of magnetic white dwarfs and neutron stars requires large data sets of atomic energy levels and transitions. Due to the huge number of computations that need to be performed to create a comprehensive database, the speed of the numerical method used is absolutely vital. In the accompanying paper [?], hereafter paper 1, we have presented an implementation of a Hartree-Fock-Roothaan method that is capable of quickly calculating energy levels and oscillator strengths for electronic systems with up to 26 electrons with good accuracy.

It is well known however, that Hartree-Fock methods are unable to treat correlation effects correctly. Methods such as full configuration interaction (Full CI) that take these effects into account on the other hand are numerically very costly and have so far only been used to create large data sets for helium [1, 2, 3] and some exemplary results for lithium and beryllium [4, 5].

Although such computationally expensive methods are not appropriate to build large data sets, it is still highly desirable to have a measure of the errors of the Hartree-Fock results. Monte Carlo methods are an ideal candidate to provide an estimate of these errors as they can use the Hartree-Fock results for the wavefunctions as input and further improve the values for the binding energies of the corresponding state. The combination of Hartree-Fock calculations with Monte Carlo methods is often used in quantum chemistry [6, 7, 8] due to its flexibility and its high accuracy that can compete with the results from Full CI. With the latter method the step from a two electron system to a three electron system is already a nontrivial task, whereas we successfully applied our method to states with up to 26 electrons.

In this paper we present our implementations of the variational quantum Monte Carlo method (VQMC) and the fixed-phase diffusion quantum Monte Carlo method [9, 10, 11] (FPDQMC) that are specifically designed to use the results from the Hartree-Fock methods presented in paper 1 as well as in the earlier references [12, 13] and have been shown to yield highly accurate results [14, 15].

The Hartree-Fock method in paper 1 in combination with the possibility to check the quality of its results with the program at hand is an ideal tool to create the large data sets of atomic energy levels and oscillator strengths needed in astrophysical applications.

We start our discussion with a general introduction of both the VQMC and the FPDQMC method in sections 2 and 3. In section 4 we compare

different ansätze for the expansion of the single-electron wave functions and the construction of trial functions. Then, in section 5, we discuss some modifications of the standard algorithm that we implemented to adapt the methods to our problem. We present a small selection of results in section 6 to compare the accuracy that we achieve with Full CI calculations, before we explain the details of the implementation and the usage of the program in section 7.

2. Variational quantum Monte Carlo

Variational methods are an important tool to gain approximate solutions of the time-independent Schrödinger equation. In order to use Monte-Carlo methods for a variational approach, we introduce the energy functional $E[\Psi]$ in the form

$$E[\Psi] = \frac{\int \Psi_G^2(\mathbf{R}) E_{L,T}(\mathbf{R}) dV}{\int \Psi_G^2(\mathbf{R}) dV}, \quad (1)$$

where

$$E_{L,T}(\mathbf{R}) = \frac{H\Psi_T(\mathbf{R})}{\Psi_T(\mathbf{R})}. \quad (2)$$

is the local energy of the trial function Ψ_T and $\Psi_G = |\Psi_T|$ is the guiding function, both of which are constructed from the approximate wave function obtained in the Hartree-Fock calculation. For details see Sec. 4. Here, $\mathbf{R} = (\mathbf{r}_1, \dots, \mathbf{r}_N)$ is a position vector in full configuration space.

VQMC uses an ensemble of W random walkers that move through the configuration space. In each step a new position \mathbf{R}' for each walker at position \mathbf{R} is proposed as $\mathbf{R}' = \mathbf{R} + \boldsymbol{\chi}$, where the components of $\boldsymbol{\chi}$ are uniform random variates. Due to the strong magnetic field, the wave functions extend much farther in z -direction than in x - and y -direction. We take this into account by choosing different intervals for the z - and the x - y -components of $\boldsymbol{\chi}$.

To ensure that the ensemble creates a statistical representation of Ψ_G^2 an acceptance-rejection step is included according to the Metropolis sampling algorithm [16, 6], i.e. the proposed step is accepted with probability

$$A(\mathbf{R}' \leftarrow \mathbf{R}) = \min \left(1, \frac{\Psi_G^2(\mathbf{R}')}{\Psi_G^2(\mathbf{R})} \right). \quad (3)$$

In general, the step size should be chosen such that the average step acceptance ratio is about 50% [6].

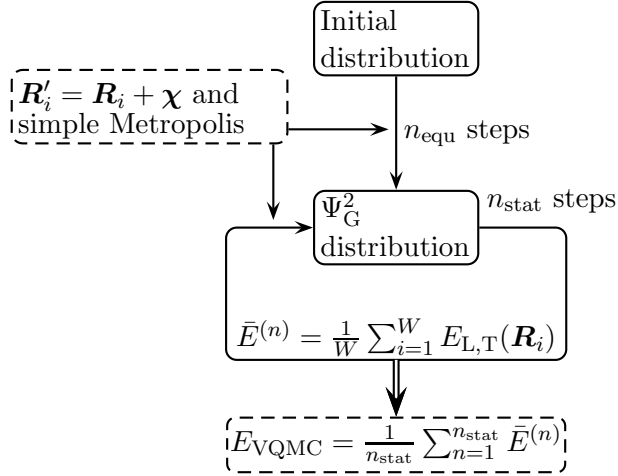


Figure 1: Course of a VQMC simulation. The simulation starts with an initial distribution of walkers. During n_{equ} equilibration steps the ensemble is distributed according to Ψ_{G}^2 . An estimate for $E[\Psi]$ is computed during the following n_{stat} steps.

Figure 1 summarizes the course of a VQMC simulation. Starting from a carefully selected initial distribution, see 5.1 for details, the ensemble moves n_{equ} equilibration steps according to this procedure after which it statistically represents Ψ_{G}^2 , before statistical data on the energies are extracted. During the following n_{stat} steps, estimates for $E[\Psi]$ are calculated by evaluating

$$\bar{E}^{(j)} = \frac{1}{W} \sum_{i=1}^W E_{\text{L,T}}(\mathbf{R}_i), \quad (4)$$

where \mathbf{R}_i is the position of the i th walker in the j th step. \bar{E}_j is the estimate for $E[\Psi]$ in the j th step. A final estimate is obtained by taking the average

$$E_{\text{VQMC}} = \frac{1}{n_{\text{stat}}} \sum_{j=1}^{n_{\text{stat}}} \bar{E}^{(j)}. \quad (5)$$

The individual estimates \bar{E} of consecutive steps are strongly correlated, since new walker positions are determined close to the old positions. This leads to a significant underestimation of the results' uncertainty if the standard deviation is computed ignoring these correlations. This effect is even stronger in FPDQMC, where the step size must be chosen much smaller than

in VQMC. As a remedy we compute the autocorrelation coefficients

$$c_i = \frac{1}{\sigma^2(n_{\text{stat}} - i)} \sum_{j=1}^{n_{\text{stat}}-i} (\bar{E}^{(j)} - E_{\text{VQMC}})(\bar{E}^{(j+i)} - E_{\text{VQMC}}), \quad (6)$$

where σ is the standard deviation of the sample of $\bar{E}^{(j)}$, and determine the correlation length l_{corr} that is defined by the criterion $c_{l_{\text{corr}}} \leq 0.1$ [17]. Then, we group the \bar{E}_j in blocks of length l_{corr} and compute the standard deviation $\sigma_{E_{\text{VQMC}}}$ of the estimate E_{VQMC} from the average block values. The same procedure is applied in FPDQMC.

2.1. Correlated Sampling

Correlations, which have a negative effect on the statistical error, can also be advantageous in VQMC if we want to evaluate $E[\Psi]$ for several similar trial functions $\{\Psi_{\text{T},i}\}$ at the same time moving only a single ensemble according to Ψ_{G} [7].

With $E_{\text{L},\text{T}}^i$ being the local energy of $\Psi_{\text{T},i}$ we can compute estimates E_{VQMC}^i simultaneously for all trial functions if we take the correction weights

$$w^i = |\Psi_{\text{T},i}|^2 / \Psi_{\text{G}}^2 \quad (7)$$

into account. These weights compensate for the fact that the ensemble is not distributed according to $|\Psi_{\text{T},i}|^2$ but according to Ψ_{G}^2 . This method works as long as the individual trial functions are not too different. Otherwise the weights in Eq. (7) can become very large for individual walkers and fluctuate strongly [18].

In addition to the saving of computer time by moving only one ensemble, the method of correlated sampling allows for the computation of the difference $\bar{E}_{\text{L}}^{(i)} - \bar{E}_{\text{L}}^{(j)}$ of the energy functionals for different trial functions with less uncertainty than with individual simulations. Explicitly, one finds for the standard deviations [7]

$$\sigma_{\Delta E_{12}}^2 = \sigma_{E_1}^2 + \sigma_{E_2}^2 - 2 \text{Cov}(E_1, E_2) < \sigma_{E_1}^2 + \sigma_{E_2}^2. \quad (8)$$

3. Fixed-phase diffusion quantum Monte Carlo

Fixed-phase diffusion quantum Monte Carlo (FPDQMC) is a variant of the diffusion quantum Monte Carlo method (DQMC) developed for the approximate treatment of complex wavefunctions [9, 10, 11], see Ref. [19] for

a recent review restricted to real wave functions. A detailed discussion of an extension of the FPDQMC method and its shortcomings can be found in Ref. [20]. In our context the FPDQMC method is a good trade-off between very high accuracy and still manageable computational cost.

DQMC is a projector method based on the simulation of the importance sampled imaginary-time ($\tau = it$) Schrödinger equation

$$\begin{aligned} \frac{\partial f(\mathbf{R}, \tau)}{\partial \tau} = & \frac{1}{2} \Delta f(\mathbf{R}, \tau) - \frac{1}{2} \nabla \cdot (f(\mathbf{R}, \tau) \mathbf{F}_Q(\mathbf{R})) \\ & - (E_L(\mathbf{R}) - E_{\text{Off}}) f(\mathbf{R}, \tau), \end{aligned} \quad (9)$$

with $f(\mathbf{R}, \tau) \equiv \Psi_G(\mathbf{R})\Psi(\mathbf{R}, \tau)$, where $\Psi(\mathbf{R}, \tau)$ is an arbitrary function. $\mathbf{F}_Q(\mathbf{R}) = 2\nabla\Psi_G(\mathbf{R})/\Psi_G(\mathbf{R})$ is the quantum force and $E_L(\mathbf{R}) = \hat{H}\Psi_G(\mathbf{R})/\Psi_G(\mathbf{R})$ the local energy.

The energy offset E_{Off} is introduced to increase the stability of the simulation and continuously adapted to the current best estimate of the true ground state energy. By expanding the function Ψ in the basis of eigenfunctions $\{\Psi_i\}$ of \hat{H} , i.e.

$$\Psi(\mathbf{R}, \tau) = \sum_{i=0}^{\infty} c_i \Psi_i(\mathbf{R}) e^{-(E_i - E_{\text{Off}})\tau}, \quad (10)$$

we see that contributions of excited states are exponentially suppressed with increasing imaginary time τ and only low-lying state parts remain after a sufficiently long interval of imaginary time. Hence, the FPDQMC method can be used to extract information, in our case the binding energy, about the lowest-lying state of a given symmetry subspace.

For the treatment with Monte Carlo, equation (9) is reformulated in integral form

$$f(\mathbf{R}', \tau + \Delta\tau) = \int G(\mathbf{R}', \mathbf{R}, \Delta\tau) f(\mathbf{R}, \tau) d^{3N}R \quad (11)$$

and the Green's function is written in short-time approximation as

$$G \approx G_D G_B + \mathcal{O}(\tau^2), \quad (12)$$

with a ‘‘drift-diffusion’’ term

$$G_D(\mathbf{R}', \mathbf{R}; \delta\tau) = (2\pi\delta\tau)^{-3N/2} \exp \left[\frac{-(\mathbf{R}' - \mathbf{R} - \delta\tau \mathbf{F}_Q(\mathbf{R})/2)^2}{2\delta\tau} \right] \quad (13a)$$

and a “branching” term

$$G_B(\mathbf{R}', \mathbf{R}; \delta\tau) = \exp \left[- \left(\frac{E_{L,G}(\mathbf{R}) + E_{L,G}(\mathbf{R}')}{2} - E_{\text{off}} \right) \delta\tau \right]. \quad (13b)$$

This integral equation can be simulated with an ensemble of random walkers in configuration space, where each walker moves according to

$$\mathbf{R} = \mathbf{R}' + \boldsymbol{\eta} + \frac{\delta\tau}{2} \mathbf{F}(\mathbf{R}'). \quad (14)$$

This movement prescription takes into account the drift-diffusion part G_D . After each step, each walker is split into

$$C = \text{trunc}(G_b(\mathbf{R}, \mathbf{R}'; \delta\tau) + \chi) \quad (15)$$

identical copies, where $\chi \in [0, 1)$ is a uniform random variate. In all following steps, these C copies move independently. If $C = 0$ the corresponding walker is deleted. This copying/deletion step takes into account the branching part G_B of the Green’s function and causes the ensemble to redistribute according to $|\Psi_G \phi_0|$, where ϕ_0 is the ground state of the corresponding symmetry subspace.

Eq. (14) violates the detailed-balance condition. To correct for that, an additional acceptance/rejection step is introduced.[7, 6] The proposed new position is accepted with probability

$$A(\mathbf{R}', \mathbf{R}, \delta\tau) = \min [1, q(\mathbf{R}', \mathbf{R}; \delta\tau)], \quad (16)$$

where

$$q(\mathbf{R}', \mathbf{R}, \delta\tau) = \frac{G_D(\mathbf{R}, \mathbf{R}'; \delta\tau) \Psi_G^2(\mathbf{R}')}{G_D(\mathbf{R}', \mathbf{R}; \delta\tau) \Psi_G^2(\mathbf{R})}. \quad (17)$$

However, this acceptance step causes only small corrections, with typical acceptance ratios $\gtrsim 99.5\%$.

In magnetic fields, the application of DQMC is complicated by the fact that the true ground state wave function may be complex. One option to treat this problem is the fixed-phase method FPDQMC, based on work by Carlson [9] and introduced by Ortiz et al. [11]. Here, the wave function is split into its modulus and its phase via

$$\Psi(\mathbf{R}, \tau) = |\Psi(\mathbf{R}, \tau)| e^{i\phi(\mathbf{R}, \tau)}. \quad (18)$$

The Schrödinger equation can then also be split into two coupled differential equations for the modulus and the phase:

$$\left(\sum_{j=1}^{N_e} -\frac{1}{2}\Delta_j + \frac{1}{2} (\nabla_j \phi + \mathbf{A}_j)^2 + V(\mathbf{r}_j) \right) |\Psi| = 0, \quad (19a)$$

$$\sum_{j=1}^{N_e} \nabla_j \cdot [|\Psi|^2 (\nabla_j \phi + \mathbf{A}_j)] = 0. \quad (19b)$$

Within the fixed-phase approximation, one assumes Eq. (19b) to be solved by the phase of Ψ_T and solves (19a) under this assumption.

By introducing FPDQMC, only G_B in equation (13b) is modified to

$$G_B(\mathbf{R}', \mathbf{R}; \delta\tau) = \exp \left[- \left(\text{Re} \left[\frac{E_{L,G}(\mathbf{R}) + E_{L,G}(\mathbf{R}')}{2} \right] - E_{\text{off}} \right) \delta\tau \right], \quad (20)$$

with $E_{L,G} = \text{Re}(E_{L,T})$. Since one does not optimize the phase of the wave function, FPDQMC cannot converge to the correct ground state energy, but one gets an excellent lower bound, i.e. the method is still variational. To estimate the remaining error in our case, we need to compare with other methods.

Figure 2 summarizes the course of a FPDQMC simulation. Although the mathematical background is much more complex, the FPDQMC implementation differs only in the way the walkers move, by the additional branching term and the slightly more complicated calculation of the energy estimate, since one has to take into account that the ensemble size $W(n)$ can be different in each step n .

In our implementation FPDQMC is always preceded by a VQMC simulation which distributes the ensemble according to Ψ_G^2 . This initial distribution allows for a fast convergence of the FPDQMC algorithm.

4. The trial functions

Manteca uses two types of single-particle wave functions from the approximate solutions of the Schrödinger equation obtained via Hartree-Fock methods. These wave functions differ in accuracy and numerical cost, i.e. the more flexible an expansion is, the larger is the numerical effort to evaluate $\Psi(\mathbf{R})$, $\nabla\Psi(\mathbf{R})$ and $\Delta\Psi(\mathbf{R})$ at a given walker position \mathbf{R} .

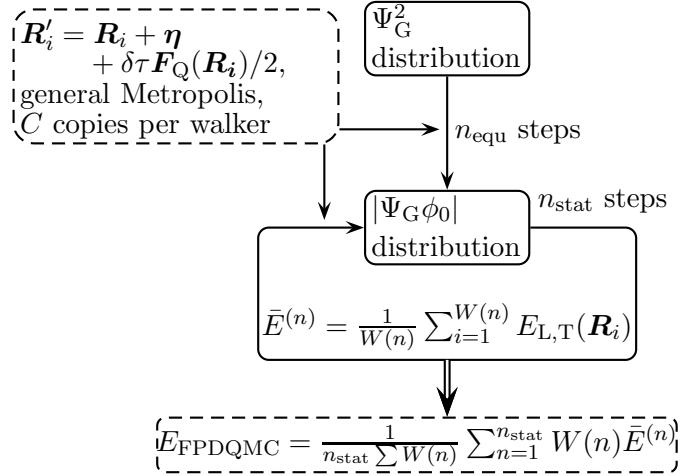


Figure 2: Course of a FPDQMC simulation. The simulation starts with an ensemble of walkers distributed according to Ψ_G^2 in a preceding VQMC simulation. The branching step ensures the redistribution according to $|\Psi_G \phi_0|$, while the Metropolis sampling step ensures detailed balance. The computation of the individual energy estimates is slightly more complicated than in VQMC as the ensemble size $W(n)$ varies from step to step.

The many-particle wave function is constructed in the most usual way [7] as a product of Jastrow factors, which are described below, and one or two Slater determinants S_\downarrow for all electrons with spin down and S_\uparrow for all electrons with spin up, which in turn are constructed from the single-electron wave functions obtained in the Hartree-Fock calculation:

$$\Psi = \mathcal{J} S_\downarrow S_\uparrow. \quad (21)$$

In case of full spin polarization S_\downarrow contains all electrons and S_\uparrow is omitted.

The most advanced single-particle ansatz from paper 1 uses individual z -wave functions for each Landau channel Φ_{nm} [21, 14] and has the form

$$\psi_{m\nu}(\mathbf{r}) = \sum_{n=0}^{N_{\text{Lan}}} P_{nm\nu}(z) \Phi_{nm}(\rho, \varphi) \quad (22)$$

for the single-electron state with quantum numbers m and ν , where ν and m denote the longitudinal excitation number and the magnetic quantum number, respectively. The individual z -wavefunctions $P_{nm\nu}$ are defined in a B -Spline basis.

The two earlier ansätze are trial functions in adiabatic approximation [22], which are defined as [23]

$$\psi_{m\nu}(\mathbf{r}) = P_{m\nu}(z)\Phi_{0m}(\rho, \varphi), \quad (23)$$

considering only contributions of the lowest Landau channel Φ_{0m} , and a less severely limited ansatz which takes 8 Landau channels into account [24, 12, 13] via

$$\psi_{m\nu}(\mathbf{r}) = P_{m\nu}(z) \sum_{n=0}^{N_L} t_{nm\nu} \Phi_{nm}(\rho, \varphi), \quad (24)$$

with $N_L = 7$ and a common z -wave function for all Landau channels.

The Slater determinants obtained from the single-particle wave functions are multiplied by Jastrow factors to include two-particle correlations [25, 26, 27] and to ensure that the wave function fulfills the cusp condition at two-particle coalescence points. We use two separately implemented Jastrow factors, one for electron-core coalescences and one for electron-electron coalescences. The electron-core Jastrow factor is implemented as

$$\mathcal{J}_{Ne} = \exp(-u_{Ne}), \quad \text{with} \quad u_{Ne} = Z \sum_{i=1}^{N_e} \frac{r_i}{1 + b_{Ne}r_i} \quad (25)$$

and the electron-electron Jastrow factor according to

$$\mathcal{J}_{ee} = \exp(-u_{ee}), \quad \text{with} \quad u_{ee} = \sum_{i=1}^{N_e} \sum_{j<i}^{N_e} \frac{a_{ij}r_{ij}}{1 + b_{ee}r_{ij}}, \quad (26)$$

where $a_{ij} = -1/4$ for electrons with parallel spin and $a_{ij} = -1/2$ for electrons with antiparallel spin. b_{Ne} and b_{ee} are free parameters that are optimized in a VQMC simulation using correlated sampling.

5. Modifications and extensions to the algorithm

The algorithm discussed so far and the construction of the wave functions from a combination of Slater determinants and Jastrow factors is fairly common. In some aspects however, we adapted the algorithm specifically to our problem.

5.1. Initialisation of the ensemble for VQMC

It is important to choose starting points for VQMC simulations in such a way that the walkers quickly find the relevant regions of the wave function. [28] A simple choice for initial positions could be, e.g., uniformly distributed points in a hypercube. Due to the very different shapes of the single-particle wave functions, a more sophisticated method has shown to be much faster and more reliable. Here, we first determine starting coordinates for each electron separately in 3-dimensional space, where the walkers are distributed randomly within $\rho \in [\rho_{\min}, \rho_{\max}]$ and z within the B -Spline basis. This initial ensemble is moved according to the Metropolis algorithm.

For maximum flexibility and reliability we equilibrate the walkers in 3-dimensional space for spin-down electrons according to the wave functions

$$\psi_{i\downarrow, \text{init}} = c_1 |\psi_{i\downarrow}| + \sum_{\substack{j=1 \\ j \neq i}}^{N_{e\downarrow}} c_0 |\psi_{j\downarrow}|, \quad (27)$$

with $c_0 = 1/\sqrt{N_{e\downarrow} + 15}$ and $c_1 = 4/\sqrt{N_{e\downarrow} + 15}$. The ansatz for spin-up electrons is chosen accordingly. The expressions for c_0 and c_1 were found empirically. The scaling factor $1/\sqrt{N_{e\downarrow} + 15}$ is chosen in such a way that the absolute value of $\psi_{i\downarrow, \text{init}}$ is approximately the same as for a normal single electron wave function. The definition of c_0 and c_1 further ensures a strong weighting of the diagonal terms in the Slater determinant but also allows for nonzero off-diagonal terms, whereas electrons with different spins are not mixed.

The final positions for all walkers for each electron can then be combined to $3N_e$ -dimensional starting positions in full configuration space.

5.2. Preparation of the guiding wave functions

A very accurate guiding function is a mixed blessing. On the one hand, we expect better results from highly precise approximations to the real solution of the Schrödinger equation. On the other hand it can be costly to numerically evaluate the wave function along with its derivatives.

The single electron wave functions defined in Eqs. (23) and (24) can be evaluated very efficiently because they feature a single z -wave function and one Landau level or a combination of Landau levels. Especially for low magnetic field strengths, where the condition $\beta \gg 1$ is not met, however, these wave function types suffer from a large loss of accuracy.

The accuracy of our results with wave functions from the ansatz (22) is significantly higher, but this ansatz requires the evaluation of individual z -wave functions for 31 Landau levels, making the computation of function values more costly roughly also by a factor of 31.

We were able to greatly increase the efficiency of our program without a significant loss of accuracy by reducing the number of Landau levels that we take into account when feasible.

Electrons with a high probability density $|\psi|^2$ close to the nucleus are strongly influenced by the Coulomb potential and therefore the cylindrical expansion (22) converges slowly and it is sensible to use the full set of Landau channels. Electrons however with high probability density far away from the core, i.e. with high excitations ν or large magnetic quantum numbers $|m|$ can be described well enough with 2 or 3 Landau levels.

Therefore, we have to remove non-significant channels before using such states in Manteca. For this task we have written the small program *refiner* that is part of the 2DLHFR package from paper 1. This program analyses the single-electron wave functions and removes Landau channels if their contributions to the binding energy are smaller than 10^{-3} Ry.

5.3. Optimization of the Jastrow factors

The free parameters b_{Ne} and b_{ee} in Eqs. (25) and (26) need to be optimized for each individual state. In the literature there exist extensive references concerning the optimization of Jastrow factors with a large numbers of free parameters, see e.g. [29, 18, 30, 31, 32, 33, 34]. With only two parameters in our case, however, a simple optimization scheme is sufficient. Here, we construct a set of wave functions with different values of (b_{Ne}, b_{ee}) , perform a VQMC simulation with correlated sampling and take the function with the lowest energy as our trial function for FPDQMC.

Figure 3 shows an example of such an optimization. The straight line represents the energy of the pure Hartree-Fock solution as trial function. The dashed line shows the results for the binding energies when an electron-core Jastrow factor is added, depending on the value of the free parameter b_{Ne} . The solid line finally shows the results with the electron-electron Jastrow factor with the best value for the parameter b_{ee} that was found in this two-dimensional optimization.

Im comparison to the results of the pure Hartree-Fock wave function, the addition of Jastrow factors causes a significant increase of the binding energy and therefore a better guiding function.

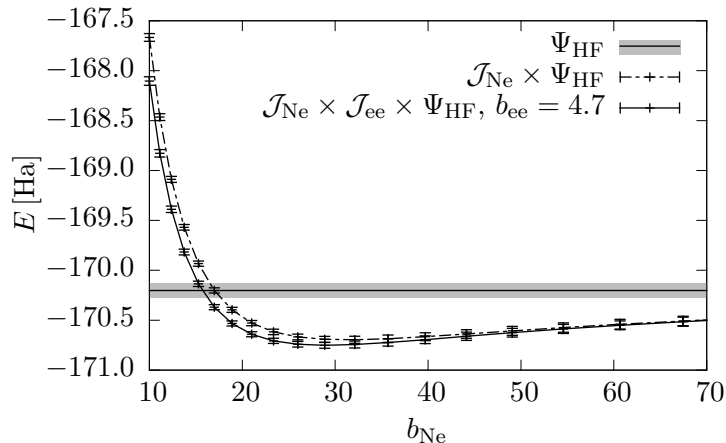


Figure 3: Jastrow factor optimization for the ground state of neon for $B = 10^7$ T.

5.4. Optimal stepsize in FPDQMC

The short-time approximation in Eq. (12) yields an error of order $\mathcal{O}(\delta\tau^2)$ but with a prefactor that strongly depends on the employed guiding function. As our algorithm should be applicable to a variety of different states for different elements and a wide range of magnetic field strengths, we need a clear criterion for a step size $\delta\tau$ such that the time-step error is negligible on the one hand and that $\delta\tau$ is as large as possible in order to minimize the correlation of the data. To minimize the time-step error in all cases, we implemented the modifications to the quantum force proposed by Umrigar et al. [35]. Here, the quantum force and the local energy are modified close to nodes of the guiding functions.

In addition to that, we found the average absolute value of the logarithm of the branching weight $\langle |\ln(G_B)| \rangle \lesssim 10^{-3}$ to be a good indicator for a suitable step size. Large branching rates imply that the trial wave function strongly deviates from the exact solution and thus indicate the possible failure of the short-time approximation. Very small branching rates, however, denote too small time steps causing large data correlations and thus bad statistics. Extensive calculations for a variety of electronic systems and with guiding functions of different qualities showed that for a value of $\langle |\ln G_B| \rangle \approx 10^{-3}$, i.e. each walker is copied or deleted in each step with a probability of approximately 0.1%, the time-step error is still negligible and, at the same time, we keep data correlations as small as possible. We implemented a routine that performs very small FPDQMC test runs to determine

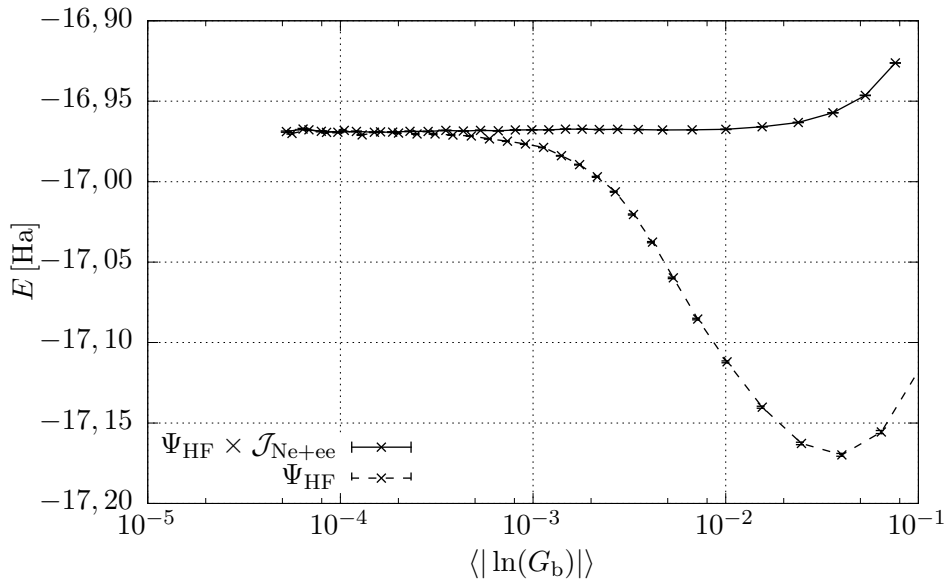


Figure 4: Results from FPDQMC calculations for the ground state of helium at $B = 5 \times 10^7$ T in dependence of different averaged absolute values of the logarithm of the branching weights $\langle |\ln G_B| \rangle$.

a step size such that the targeted average branching rate is matched.

An example of the dependence of the energy results on the value of $\langle |\ln(G_B)| \rangle$ is shown in Fig. 4. There, we compare the energies when we use the Hartree-Fock solution alone as trial function and the energies when Jastrow factors are added and the Umrigar correction algorithm is used. In the latter case, the energy results are stable for $\langle |\ln G_B| \rangle \leq 10^{-2}$, whereas the energies of the pure Hartree-Fock guiding function do not converge up to $\langle |\ln G_B| \rangle \approx 7 \times 10^{-4}$. This shows that especially the Jastrow factors cause a large reduction of the time-step error. Smaller values of $\langle |\ln(G_B)| \rangle$ obviously correspond to smaller time steps.

5.5. Aging walkers

In rare cases, it can happen in FPDQMC that a walker gets stuck at a certain position in configuration space without an appreciable chance of leaving it again. Umrigar et. al. [35] coined the term “persistent configuration” for this phenomenon. Such a walker can cause the simulation to crash if its branching weight is larger than 1 at its position because it will create copies that are also stuck and will also create copies such that after a few steps this

walker dominates the ensemble. To avoid such a phenomenon, we introduce a walker age a_W , an approach similar to the one proposed in Ref. [35]. The walker age is defined as the number of consecutive steps in which it did not move. We leave walkers with ages 0 and 1 unchanged but prevent walkers with $a_W \geq 2$ from branching by changing their branching weight to

$$G_B = \exp[-0,1(a_W - 2)]. \quad (28)$$

This causes these walkers to be deleted very quickly and prevents a disturbing influence on the simulation. Of course, the age is inherited to all copies of this walker. At the same time this is only a minimal modification of the algorithm that does not cause an error of any significance because of the high acceptance ratios in FPDQMC above 99.5%.

6. Results and accuracies

Quantum Monte Carlo methods are generally very accurate. We thoroughly discussed the accuracy of the results obtained with our FPDQMC implementation in Ref. [14]. There, we compared our results for several helium states to Full CI calculations by Becken et al.[1] and Becken and Schmelcher[2, 3]. Their values represent the most accurate values for the binding energies of helium in strong magnetic fields that we know of.

Table 1 shows our results for the high-field ground state and the first excited state of the corresponding symmetry subspace for helium, lithium and beryllium for several magnetic field strengths compared with results from Full CI calculations [2, 4, 5].

We compute a slightly lower binding energy for the helium and lithium ground state, but higher binding energies for the beryllium ground state. It is remarkable that for low magnetic field strengths, where the 2DLHFR results already lose some accuracy, FPDQMC improves the binding energies by several percent and even here reaches a very high level of accuracy.

Our results for the excited states are not strictly variational, but are still in good agreement with the Full CI values. This strongly hints on our trial functions for the excited states being almost orthogonal to the ground states, which in general makes FPDQMC computations for excited states possible [19].

The strength of our FPDQMC approach, next to its accuracy that is comparable to Full CI results, is its high flexibility concerning the number

Table 1: FPDQMC results for helium, lithium and beryllium. We compare our results for the high-field ground state and the first excited state in the corresponding symmetry subspace with results from Full-CI calculations by Becken and Schmelcher [2] and Al-Hujaj and Schmelcher [4, 5]. The states are labelled using the single-electron notation $-m^\nu$ described in paper 1.

helium						
β	$0^0 1^0$			$0^0 1^2$		
	FPDQMC	2DHFR	Ref. [2]	FPDQMC	2DHFR	Ref. [2]
0,25	2,61727(14)	2,517	2,620021	2,34637(13)	2,239	2,348197
0,40	2,83353(11)	2,772	2,835619	2,49015(12)	2,420	2,486853
0,50	2,96359(11)	2,913	2,965504	2,57346(10)	2,519	2,572178
0,80	3,30747(8)	3,273	3,308774	2,80085(8)	2,770	2,802301
1,00	3,50749(7)	3,478	3,508911	2,93732(7)	2,912	2,938822
2,50	4,62438(6)	4,606	4,625491	3,72013(5)	3,705	3,718569
5,00	5,83810(6)	5,822	5,839475	4,58415(5)	4,574	4,582689
10,00	7,43933(6)	7,422	7,440556	5,73246(4)	5,724	5,731115
25,00	10,28293(7)	10,261	10,2841	7,77844(5)	7,771	7,777100
50,00	13,10334(11)	13,073	13,10478	9,80789(6)	9,801	9,806638
lithium						
β	$0^0 1^0 2^0$			$0^0 1^0 2^2$		
	FPDQMC	2DHFR	Ref. [4]	FPDQMC	2DHFR	Ref. [4]
1,0	7,52702(24)	7,398	7,530125	7,03553(22)	6,911	7,038917
2,5	9,58838(14)	9,529	9,591769	8,79881(14)	8,745	8,799910
5,0	11,95495(11)	11,910	11,957294	10,84041(11)	10,805	10,841017
beryllium						
β	$0^0 1^0 2^0 3^0$			$0^0 1^0 2^0 3^2$		
	FPDQMC	2DHFR	Ref. [5]	FPDQMC	2DHFR	Ref. [5]
1,0	13,1731(7)	12,759	13,1762	12,7250(7)	12,317	12,7321
2,5	16,3213(4)	16,154	16,3139	15,5954(4)	15,434	15,5887
5,0	20,0402(3)	19,940	20,0242	19,0093(3)	18,918	18,9887

of electrons. Already for beryllium as a four electron system we outmatch the Full CI approach which reaches its limits there due to a rapidly growing base size.[5] On the other hand, FPDQMC in conjunction with 2DHLFR is capable of treating systems with up to 26 electrons with reasonable accuracy.

It remains to be noted that a higher level of accuracy than which we can reach with the 2DLHFR-FPDQMC combination is probably not of vital importance in the context of astrophysical applications, especially in the investigation of neutron stars, where the observed X-ray spectra have quite large inaccuracies and a low spectral resolution, see e.g. [36].

7. Program description

The Manteca program has been documented using doxygen.[37] Details on the implementation can be looked up in this documentation and we only give a brief overview here.

We use Lapack routines for the computation of the Slater determinants and the SLATEC library for the evaluation of B -Splines. The wavefunctions are implemented in a hierarchical structure. On the base level we have the single-electron wave functions that we construct from the Hartree-Fock results and the Jastrow factors. Finally, the trial function is constructed from these constituents via objects representing mathematical functions, i.e. product, Hartree product and Slater determinant. The single electron wave functions for all electrons of spin down and spin up, respectively, are combined in separate Slater determinants. These two determinants are combined in a Hartree product and finally we add the Jastrow factors and the Hartree product to a normal product. We use the `boost::shared_ptr` construct that is now part of the C++11 standard for a safe and efficient implementation of this structure.

7.1. State files

Manteca uses the file ending of the state files to decide whether the current Hartree Fock trial function is described in the full two dimensional basis of Eq. (22) (`ac1b`) or in the simpler expansions given in Eqs. (23) and (24) (`aib`). The structure of the state files is described in detail in the documentation.

7.2. Options

Manteca can be operated by providing options either via an ini-file or on the command line or by a combination of both methods, where options given on the command line overwrite those in an ini-file.

`help` Shows a list of all available options and their descriptions.

To start a first calculation, the user should at least provide the following options:

`p <file>` Manteca will use the state file `<file>`.

`L <file>` Manteca will use all state files given in the list `<file>` and consecutively perform all calculations for them.

`dqmc` Manteca will make a FPDQMC simulation. By default it only performs VQMC.

`dqmc_tau` Step size $\delta\tau$ for FPDQMC. If a proper step size is unknown, an optimization is recommended that will use this value as starting point.

`optimize_lnGB` This option starts such an optimization of the step size. The value of $\langle |\ln G_B| \rangle$ that Manteca tries to reach can be modified with `lnGB_desired <value>`

`n_walkers <number>` Number of walkers. Small rounding errors can occur here as the walkers are evenly distributed on all available nodes.

The accuracy of the results can be significantly improved when Jastrow factors are used. These are added with the following options:

`jastrow_opt` Optimize the b -parameters for the Jastrow factors and then add these factors to the guiding function. This option must be used together with the options

`JMax <MaxNuc> <MaxEE>`, `JMin <MinNuc> <MinEE>` that provide the search intervals for b_{Ne} and b_{ee} .

If good b parameters are already known, Jastrow factors can be directly added via

`use_nuc_jastrow ` Adds an electron-core Jastrow factor with parameter `b` to the trial function.

`use_EE_jastrow ` Adds an electron-electron Jastrow factor with parameter `b` to the trial function.

This allows the user to divide the task of optimizing the wave function and computing binding energies with it into smaller calculations. This is useful on environments where CPU time is strictly limited.

Sometimes it can be useful to be able to exactly reproduce a simulation. Normally, Manteca's random number generator is initialised with the system time t in seconds (and $t+n$ on other nodes, where n is the nodes number), but it is also possible to explicitly provide a seed with the `seed <seed>` option. Manteca prints the seed for each simulation into the results file. With the same seed on the same number of nodes, Manteca will always obtain exactly the same result.

7.3. An example calculation

The ini-file `example.ini` provides Manteca with instructions to compute the binding energy for the helium ground state in a magnetic field of $B = 10^7$ T on a single core in about 30 minutes. As we explicitly provide a fixed seed, the result of this computation should always be an estimate of $E = 9.71268(72)$ Ha. To start a computation with this file the user should change to the folder where manteca has been compiled and type in the following command:

```
seriell/manteca -p example/heliumGSB21.2719-r.aclb -ini example/Example.ini
```

The uncertainty of the results of a Monte Carlo simulation decreases as $1/\sqrt{N}$ with the number N of independent estimates and the numerical effort to evaluate the wave function grows approximately as N_e^2 with the number of electrons, because the dominant factor is the evaluation of the single-electron wave functions and not the computation of the Slater determinant which grows $\sim N_e^3$.

Hence, except for relatively simple examples with 2-3 electrons and relatively low precision, simulations take unacceptably long on a single processor.

A parallel computation can be started quite similarly to the single core case with the command

```
mpirun -hostfile <hostfile> parallel/manteca <instructions>
```

7.4. Output files

Manteca puts all output in a folder `Output` that is a subfolder of the location where it is executed. This folder is not created if it does not exist.

The output of Manteca is written to several files. The results of the VQMC and the FPDQMC calculations are written to corresponding files in the simple form $E(\sigma)$, i.e. the given energy value followed by the standard deviation in parantheses. The results of both calculations together with the step size $\delta\tau$ used in FPDQMC, the resulting value of $\langle |\ln(G_B)| \rangle$, the average acceptance ratio and the correlation length, as well as the number of deleted and copied walkers is additionally written to a file giving a compact overview over the simulation. Finally, all output to standard output and error streams is written to a detailed output file.

8. Acknowledgements

This work was supported by bwGRiD [38], a member of the German D-Grid initiative.

- [1] W. Becken, P. Schmelcher, F. K. Diakonov, The helium atom in a strong magnetic field, *J. Phys. B* 32 (1999) 1557 – 1584.
- [2] W. Becken, P. Schmelcher, Non-zero angular momentum states of the helium atom in a strong magnetic field, *J. Phys. B* 33 (3) (2000) 545.
- [3] W. Becken, P. Schmelcher, Higher-angular-momentum states of the helium atom in a strong magnetic field, *Phys. Rev. A* 63 (2001) 053412.
- [4] O. Al-Hurjaj, P. Schmelcher, Lithium in strong magnetic fields, *Phys. Rev. A* 70 (3) (2004) 033411.
- [5] O. Al-Hurjaj, P. Schmelcher, Beryllium in strong magnetic fields, *Phys. Rev. A* 70 (023411) (2004) 023411.
- [6] W. M. C. Foulkes, L. Mitas, R. J. Needs, G. Rajagopal, Quantum Monte Carlo simulations of solids, *Rev. Mod. Phys.* 73 (1) (2001) 33 – 83.
- [7] B. L. Hammond, W. A. Lester Jr., P. J. Reynolds, Monte Carlo Methods in ab initio quantum chemistry, World Scientific Lecture and Course Notes in Chemistry, World Scientific Publishing Co. Pte. Ltd., Singapur, 1994.
- [8] L. K. Wagner, Quantum monte carlo for ab initio calculations of energy-relevant materials, *International Journal of Quantum Chemistry* (2013) n/a–n/a.

- [9] J. Carlson, Green's function Monte Carlo study of light nuclei, *Phys. Rev. C* 36 (5) (1987) 2026–2033.
- [10] G. Ortiz, M. D. Jones, D. M. Ceperley, Ground state of a hydrogen molecule in superstrong magnetic fields, *Phys. Rev. A* 52 (1995) R3405 – R3408.
- [11] G. Ortiz, D. M. Ceperley, R. M. Martin, New Stochastic Method for Systems with Broken Time-Reversal Symmetry: 2D Fermions in a Magnetic Field, *Phys. Rev. Lett.* 71 (17) (1993) 2777 – 2780.
- [12] D. Engel, G. Wunner, Hartree-Fock-Roothaan calculations for many-electron atoms and ions in neutron star magnetic fields., *Phys. Rev. A*. 78 (2008) 032515.
- [13] C. Schimeczek, D. Engel, G. Wunner, A highly optimized code for calculating atomic data at neutron star magnetic field strengths using a doubly self-consistent Hartree-Fock-Roothaan method, *Comp. Phys. Comm.* 183 (2012) 1502 – 1510.
- [14] C. Schimeczek, S. Boblest, D. Meyer, G. Wunner, Atomic ground states in strong magnetic fields: Electron configurations and energy levels, *Phys. Rev. A* 88 (2013) 012509.
- [15] S. Boblest, C. Schimeczek, G. Wunner, Ground states of helium to neon and their ions in strong magnetic fields, *Phys. Rev. A* 89 (2014) 012505.
- [16] N. Metropolis, A. W. Rosenbluth, M. N. Rosenbluth, A. M. Teller, E. Teller, Equations of State Calculations by Fast Computing Machines, *J. Chem. Phys.* 21 (1953) 1087–1092.
- [17] M. D. Jones, G. Ortiz, D. M. Ceperley, Released-phase quantum Monte Carlo method, *Phys. Rev. E* 55 (5) (1997) 6202 – 6210.
- [18] P. R. C. Kent, R. J. Needs, G. Rajagopal, Monte Carlo energy and variance-minimization techniques for optimizing many-body wave functions, *Phys. Rev. B* 59 (1999) 12344–12351.
- [19] A. Lüchow, Quantum Monte Carlo methods, *Comput. Mol. Sci.* 1 (2011) 388 – 402.

- [20] F. A. Reboredo, Many-body calculations of low-energy eigenstates in magnetic and periodic systems with self-healing diffusion Monte Carlo: Steps beyond the fixed phase, *J. Chem. Phys.* 136 (2012) 204101.
- [21] C. Schimeczek, 2D Hartree-Fock-Roothaan calculations for atoms and ions in neutron star atmospheres., Ph.D. thesis, Universität Stuttgart (2013).
- [22] L. I. Schiff, H. Snyder, Theory of Quadratic Zeeman-Effect, *Phys. Rev.* 55 (1939) 59 – 63.
- [23] D. Engel, M. Klews, G. Wunner, A fast parallel code for calculating energies and oscillator strengths of many-electron atoms at neutron star magnetic field strengths in adiabatic approximation, *Comp. Phys. Comm.* 180 (2) (2009) 302–311.
- [24] D. Engel, Hartree-Fock-Roothaan-Rechnungen für Vielelektronen-Atome in Neutronenstern-Magnetfeldern, Ph.D. thesis, Universität Stuttgart (2007).
- [25] T. Kato, On the Eigenfunctions of Many-Particle Systems in Quantum Mechanics, *Comm. Pure Appl. Math.* 10 (1957) 151 – 177.
- [26] C. A. Coulson, A. H. Neilson, Electron Correlation in the Ground State of Helium, *Proc. Phys. Soc.* 78 (1961) 831 – 837.
- [27] R. T. Pack, W. B. Brown, Cusp Conditions for Molecular Wavefunctions, *J. Chem. Phys.* 45 (1966) 556 – 559.
- [28] D. R. Fisher, D. R. Kent, M. T. Feldmann, W. A. Goddard III, An Optimized Initialization Algorithm to Ensure Accuracy in Quantum Monte Carlo Calculations, *J. Comp. Chem.* 29 (14) (2008) 2335 – 2343.
- [29] C. Huang, C. J. Umrigar, M. P. Nightingale, Accuracy of electronic wave functions in quantum Monte Carlo: The effect of high-order correlations, *J. Chem. Phys.* 107 (8) (1997) 3007 – 3013.
- [30] M. P. Nightingale, V. Melik-Alaverdian, Optimization of Ground- and Excited State Wave Functions and van der Waals Clusters, *Phys. Rev. Lett.* 87 (4) (2001) 043401.

- [31] N. D. Drummond, M. D. Towler, R. J. Needs, Jastrow correlation factor for atoms, molecules, and solids, *Phys. Rev. B* 70 (2004) 235119.
- [32] C. J. Umrigar, J. Toulouse, C. Filippi, S. Sorella, R. G. Hennig, Alleviation of the Fermion-Sign Problem by Optimization of Many-Body Wave Functions, *Phys. Rev. Lett.* 98 (2007) 110201.
- [33] J. Toulouse, C. J. Umrigar, Full optimization of Jastrow-Slater wave functions with application to the first-row atoms and homonuclear diatomic molecules, *J. Chem. Phys.* 128 (2008) 174101.
- [34] H. Luo, Complete optimisation of multi-configuration Jastrow wave functions by variational transcorrelated method, *J. Chem. Phys.* 135 (2011) 024109.
- [35] C. J. Umrigar, M. P. Nightingale, K. J. Runge, A diffusion Monte Carlo algorithm with very small time-step errors, *J. Chem. Phys.* 99 (4) (1993) 2865 – 2890.
- [36] G. F. Bignami, A. De Luca, P. A. Caraveo, S. Mereghetti, M. Moroni, R. P. Mignani, M. Marconi, 1E1207.4-5209 - a Unique Object, *Mem. S. A. It.* 75 (3) (2004) 448.
- [37] D. van Heesch, Doxygen—Generate documentation from source code, <http://www.stack.nl/~dimitri/doxygen/index.html>.
- [38] bwGRiD, Member of the German D-Grid initiative, funded by the Ministry of Education and Research (Bundesministerium für Bildung und Forschung) and the Ministry for Science, Research and Arts Baden-Wuerttemberg (Ministerium für Wissenschaft, Forschung und Kunst Baden-Württemberg), <http://www.bw-grid.de>, Tech. rep., Universities of Baden-Württemberg (2007-2013).